Cross wavelet, coherence and phase between water surface temperature and heat flux in a tropical hydroelectric reservoir

E.H. Alcântara[*], J.L. Stech, J.A. Lorenzzetti, E.M.L.M. Novo

National Institute for Space Research, Remote Sensing Division, Brazil.

*Corresponding author, e-mail enner@dsr.inpe.br

ABSTRACT

Water temperature plays an important role in ecological functioning and in controlling the biogeochemical processes of a water body. Conventional water quality monitoring is expensive and time consuming. It is particularly problematic if the water bodies to be examined are large. Conversely, remote sensing is a powerful tool to assess aquatic systems. The objective of this study was to analyze the time series of surface water temperature and heat flux to improve understanding of temporal variations in a hydroelectric reservoir. In this work, MODIS land-surface temperature (LST) level 2, 1-km nominal resolution data (MOD11L2, version 5) were used. All available clear-sky MODIS/Terra images from 2003 to 2008 were used, resulting in a total of 786 daytime and 473 nighttime images. Time series of surface water temperature was obtained by the monthly mean 3x3 window of three area of the reservoir: (1) first near the dam, (2) in the centre of the reservoir and (3) in the confluence of the rivers. Long-term environmental time series of continuously collected data are fundamental to identify and classify pulses and determining their role in aquatic systems. In-situ meteorological variables were used from 2003 to 2008 to calculate the surface energy budget time series. A correlation between daytime and nighttime surface water temperatures and the computed heat fluxes were made. The influence of the correlated heat flux in the water temperature was analyzed using the Cross-wavelet, coherence and phase analysis.

KEYWORDS
MODIS/Terra, hydroelectric reservoir, physical limnology.

INTRODUCTION
Research about water quality of reservoirs and lakes has been based mostly on point station datasets or along track lines obtained during cruises (Jerosch et al., 2006). High quality in situ measurements of water parameters are usually limited, and they are particularly critical for time series data and key variables. The detection of trends and sudden changes in the aquatic system is dependent on both the availability of long-term time series of environmental data and their proper analysis (Alcântara et al. 2010).
The objective of this paper is to analyze the time series of water surface temperature and heat balance of a tropical hydroelectric reservoir derived from satellite data.

STUDY AREA
The Itumbiara hydroelectric reservoir (18°25'S, 49°06'W) is located in a region stretched between Minas Gerais and Goiás States (Central Brazil) that was originally covered by tropical grassland savanna. The damming of the Parnaiba River flooded its main tributaries: the Araguari and Corumbá rivers. The basin's geomorphology resulted in a lake with a

dendritic pattern covering an area of approximately 814 km² and a volume of 17.03 billion m³ (Figure 1).
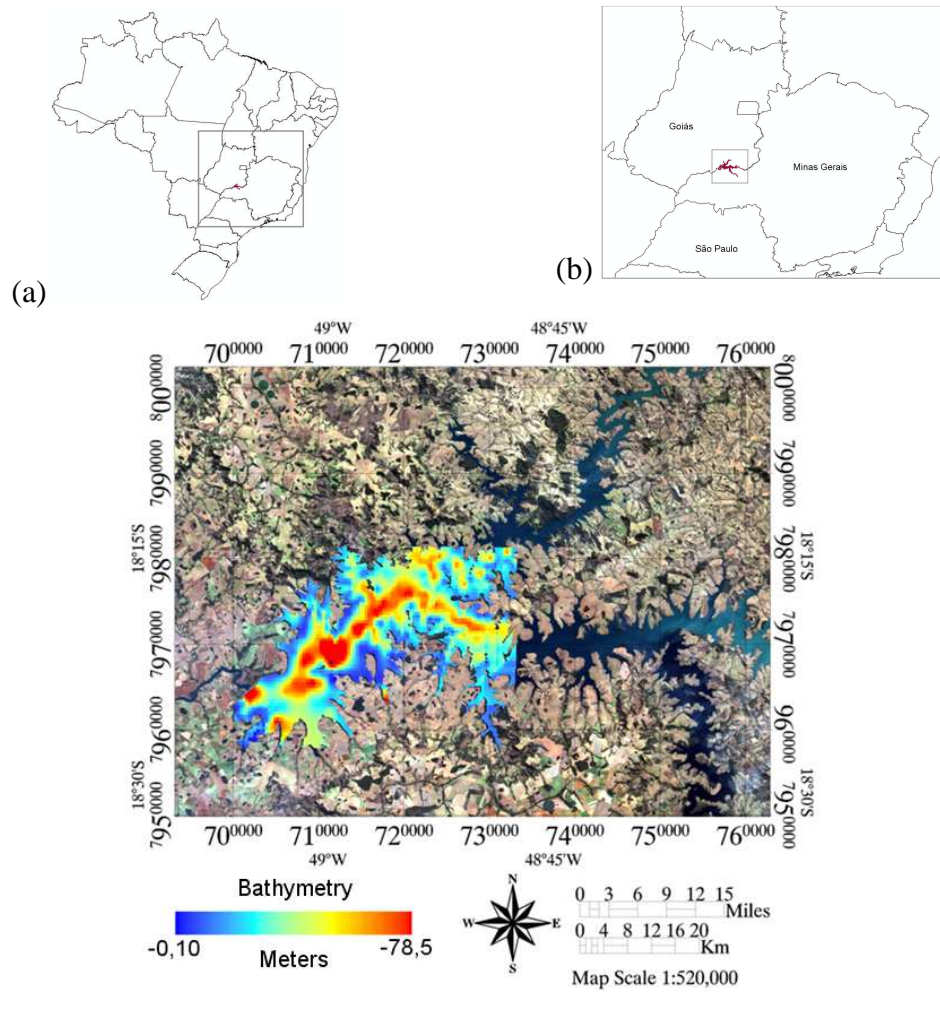

(a)

(b)

(c)

Figure 1: Localization of Itumbiara hydroelectric reservoir in Brazil's central area (a), at the state scale (b) and at the regional scale (c) with the bathymetric map.

METHODOLOGICAL APPROACH

Satellite data

MODIS water surface temperature (WST) level 2, 1-km nominal resolution data (MOD11L2, version 5) were obtained from the National Aeronautics and Space Administration Land Processes Distributed Active Archive Center (Wan, 2008). All available clear-sky MODIS Terra imagery between 2003 and 2008 were selected by visual inspection, resulting in a total of 786 daytime images and 473 nighttime images. A shoreline mask to isolate land from water was built using the TM/Landsat-5 image in order to isolate some anomalously cold or warm pixels remaining at some locations near the shoreline of the reservoir.

The WST-MODIS data were extensively validated for inland waters and were considered accurate (Oesch et al., 2005; Oesch et al., 2008; Reinart and Reinhold, 2008; Crosman and Horel, 2009).

Surface Energy Budget

A study of the energy exchange between the lake and atmosphere is essential for understanding the aquatic system behavior and its reaction to possible changes of environmental and climatic conditions (Bonnet, Poulin and Devaux, 2000). The exchange of heat across the water surface was computed using the methodology described by Henderson-Sellers (1986) as:

$$\phi_N = \phi_s(1-A) - (\phi_{ri} + \phi_{sf} + \phi_{lf}) \tag{1}$$

where ϕ_N is the surface heat flux balance, ϕ_s is the incident short-wave radiation, A is the albedo of water (=0.07), ϕ_{ri} is the Longwave flux, ϕ_{sf} is the sensible heat flux and ϕ_{lf} is the latent heat flux. The units used for the terms in Eq. (1) are W m^{-2}.

Time Series

The time series was constructed using the results obtained from the satellite imagery through the sampling in three regions of the reservoir (a window of $\overline{3x3}$). The figure 2 shows the regions where these sampling was taken.
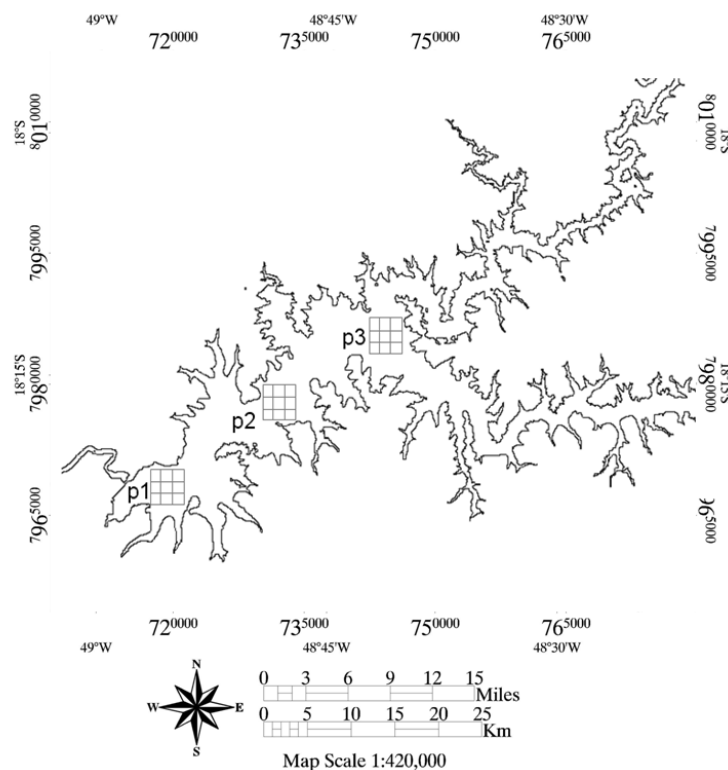

Figure 2: Sampling points location: p1 – region near de dam; p2 – central region of the reservoir and p3 – region under influence of the rivers.

Time Series Analysis

To show the relationship between WST and the significantly time series highlighted by Pearson's correlation the cross wavelet analysis was carried out and the coherence and phase analyzed (Grinsted, 2004).

The cross wavelet transform of two time series x_n and y_n is defined as $W^{xy} = W^x W^{y*}$, where $*$ denotes complex conjugation, so the cross wavelet power could be defined as $\left|W^{xy}\right|$ (Grinsted et al. 2004). The interpretation of complex argument $\arg(W^{xy})$ can be interpreted

as the local relative phase between x_n and y_n in time frequency space. The cross wavelet power theoretical distribution of two time series with background power spectra P_k^x and P_k^y is given in Torrence and Compo (1998) as:

$$D\left(\frac{\left|W_n^x(s)W_n^{y^*}(s)\right|}{\sigma_x\sigma_y} < p\right) = \frac{Z_v(p)}{v}\sqrt{P_k^x P_k^y} \tag{2}$$

where $Z_v(p)$ is the confidence level associated with the probability p for a pdf defined by the square root of the product of two χ^2 distributions. Cross wavelet power reveals areas with high common power.

Another useful measure is how coherent the cross wavelet is in time frequency space. The wavelet coherence could be defined following Torrence and Webster (1998) as:

$$R_n^2(s) = \frac{\left|S(s^{-1}W_n^{wy}(s))\right|^2}{S(s^{-1}\left|W_n^x(s)\right|^2).S(s^{-1}\left|W_n^y(s)\right|^2)} \tag{3}$$

where S is a smoothing operator; Notice that this definition closely resembles that of a traditional correlation coefficient, and is useful to think of the wavelet coherence as a localized correlation coefficient in time frequency space. The calculation procedures of cross wavelet and wavelet coherence were coded in Matlab 6.5 (The MathWorks, Inc., Natick, MA).

RESULTS
Statistical model for daytime and nighttime water surface temperatures
The Pearson correlation computed between the daytime and nighttime WST derived from the MODIS image against the heat flux terms is shown in Table 1. For daytime temperatures, the only significant correlated heat flux was the shortwave radiation; for nighttime temperatures, it was the longwave radiation, latent heat flux and sensible heat flux.

The multiple regression analysis shows that for daytime WST, the correlated heat flux terms explain 89% of the annual variation (RMS=0.89°C, $\rho < 0.0013$). For nighttime, the heat flux terms explain 94% (RMS=0.53°C, $\rho < 0.0002$). The representative equations of these relationships are presented in equations 2 and 3:

$$T_{daytime} = 18.78 + (0.02\phi_S) \tag{2}$$

$$T_{nighttime} = 38.17 - (0.31\phi_{ri}) + (0.55_{lf}) + (0.39\phi_{sf}) \tag{3}$$

where $T_{daytime}$ is the daytime water surface temperature (°C), $T_{nighttime}$ is the nighttime water surface temperature (°C), ϕ_s is the short wave radiation (Wm^{-2}), ϕ_{ri} is the long wave radiation (Wm^{-2}), ϕ_{lf} is the latent flux (Wm^{-2}) and ϕ_{Sf} is the sensible flux (Wm^{-2}).

Table 1: Pearson correlation coefficients for daytime and nighttime surface temperatures against shortwave radiation (ϕ_S), longwave radiation (ϕ_{ri}), sensible flux (ϕ_{sf}), and latent flux (ϕ_{lf}).

	Daytime water temperature	Nighttime water temperature
ϕ_S	0.64	-
ϕ_{ri}	-	-0.65
ϕ_{sf}	-	0.42
ϕ_{lf}	-	-0.64

Only values at a 95% significance level are shown.

Only the incoming shortwave radiation was needed to model the daytime WST. This is because when the shortwave radiation increases, the air temperature increases and transfers heat in the water column. However, the pattern of wind intensity and direction during the day is also important; with high wind intensity, the surface water loses heat through convection.
At night, the processes of convection and advection acting at the surface water and the balance of longwave radiation are important to drive the water temperature. Because of this, equation 3 is a subtraction of the joint effects of these three important fluxes.

Cross wavelet, coherence and phase
Daytime water surface temperature versus shortwave radiation (ϕ_S)

The cross wavelet between the daytime WST and the ϕ_S shows two band period of high common power: the first in the band period of 4.5-7 (regions 1 and 2) months, in special the semester from years 2004 and 2007; the second with the highest common power between 9-15 months (region 3) also with special attention in the years 2004 and 2007 (Figure 3-a).
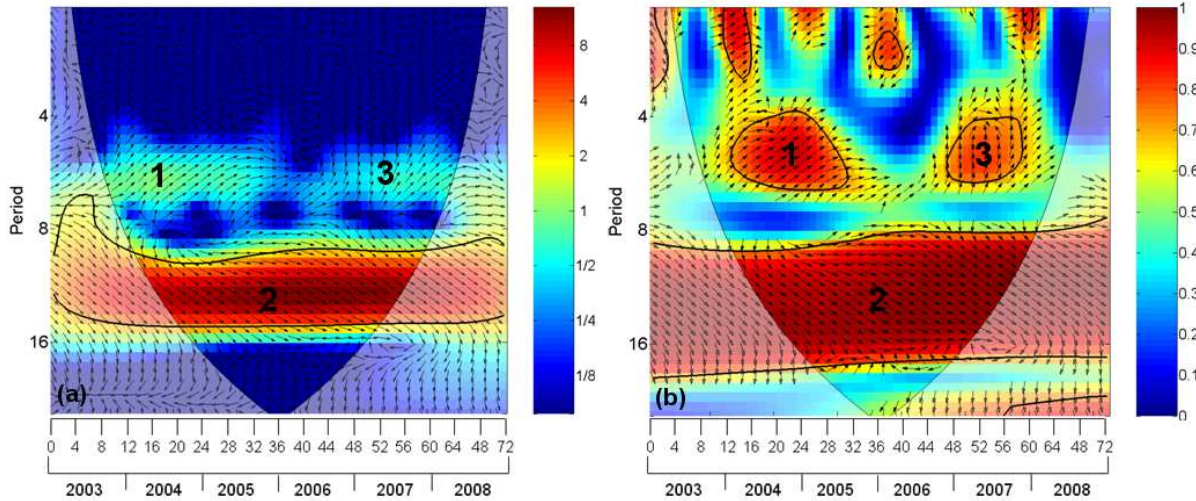

Figure 3: Cross wavelet between daytime WST and ϕ_S (a) and the coherence and phase (b).

The coherence in these common power periods (Figure 3-b) that: for the region 1 (period of 4-7 months) the ϕ_S is retarded 45º [~21 days] in relation to WST (from January 2004 to July 2005); for the region 2 (period of 8-16.5 months) the ϕ_S is advanced 45º [~1.5 months] in relation to WST and the region 3 (band period of 4.5-6.5) the ϕ_S is retarded 90º [~1.25 months] in relation to WST.

Nighttime water surface temperature versus longwave radiation (ϕ_{ri})

The cross wavelet analysis between the nighttime WST and ϕ_{ri} is show in the Figure 4. Five high common power was identified: (1) band period of 1-2 months localized between November 2004 and April 2005 (Figure 4-a), with ϕ_{ri} advanced 45º [~ 6 days] in relation to nighttime WST (Figure 4-b); (2) band period of 3-4 months localized between January and July 2007, with ϕ_{ri} advanced 90º [~27 days]; (3, 4) band period of 5-6 months end of 2005 until the beginning of 2006, with ϕ_{ri} advanced 135º [~2 months]; and (5) band period of 9-15 months localized between January 2004 until November 2007, with ϕ_{ri} advanced 135º [~6 months].
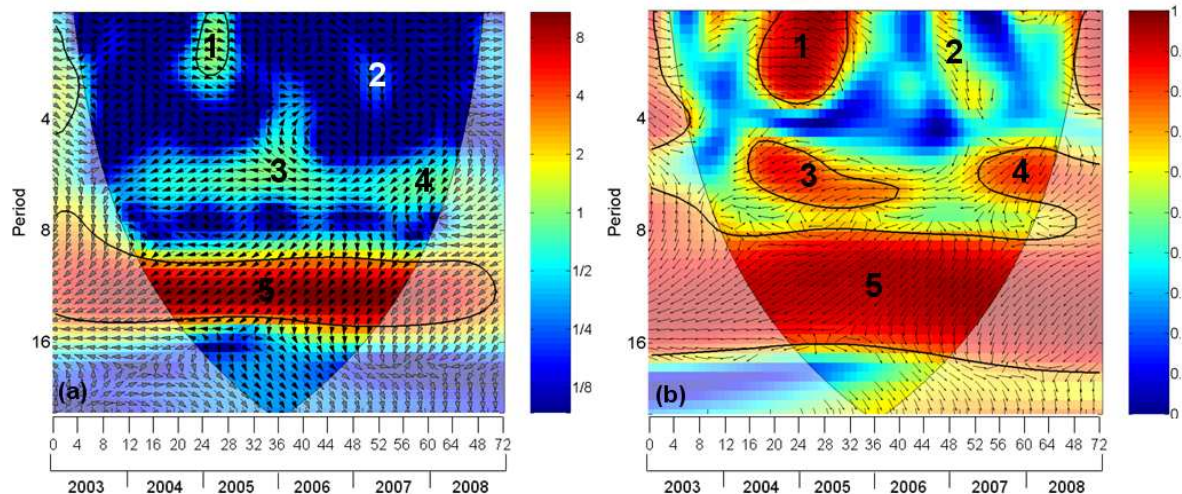

Figure 4: Cross wavelet between nighttime WST and ϕ_{ri} (a) and the coherence and phase (b).

Nighttime water surface temperature versus sensible flux (ϕ_{sf})

The cross wavelet analysis between the nighttime WST and ϕ_{sf} is show in the Figure 5. Four high common power was identified: (1) band period of 2-3 months localized from September to December 2004 (Figure 5-a), with ϕ_{sf} retarded 45º [~9 days] in relation to nighttime WST (Figure 5-b); (2) band period of 5-7 months localized from April 2004 to April 2005, with ϕ_{sf} advanced 135º [~2 months]; (3) band period of 5.5-7 months between May 2007 to March 2008, with ϕ_{sf} advanced 135º [~2 months]; and (4) band period of 9-15 months localized between February 2004 until November 2007, with ϕ_{ri} advanced 45º [~2 months].
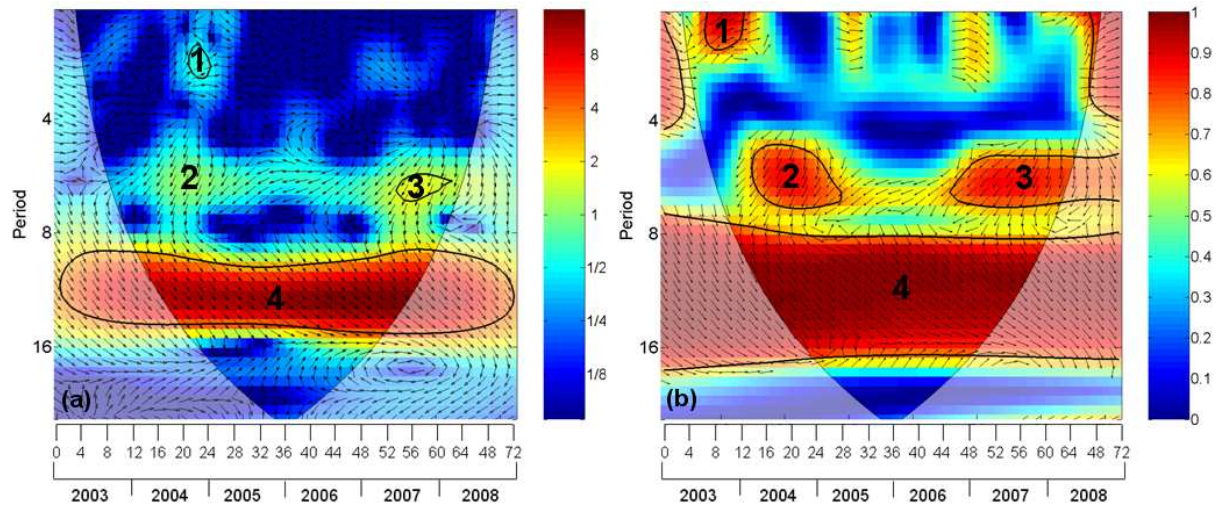
Figure 5: Cross wavelet between nighttime WST and ϕ_{sf} (a) and the coherence and phase (b).

Nighttime water surface temperature versus latent flux (ϕ_{lf})

The cross wavelet analysis between the nighttime WST and ϕ_{lf} is show in the Figure 6 and was identified four high common: (1) band period of 1-3 months localized from August 2004 to April 2005 (Figure 6-a), with ϕ_{lf} retarded 45º [~8 days] in relation to nighttime WST (Figure 6-b); (2, 3) band period of 6-8 months localized from April 2004 to January 2005, with ϕ_{lf} retarded 90º [~1.7 months]; (4) band period of 9-15 months between February 2004 to November 2007, with ϕ_{lf} and nighttime WST in anti-phase.
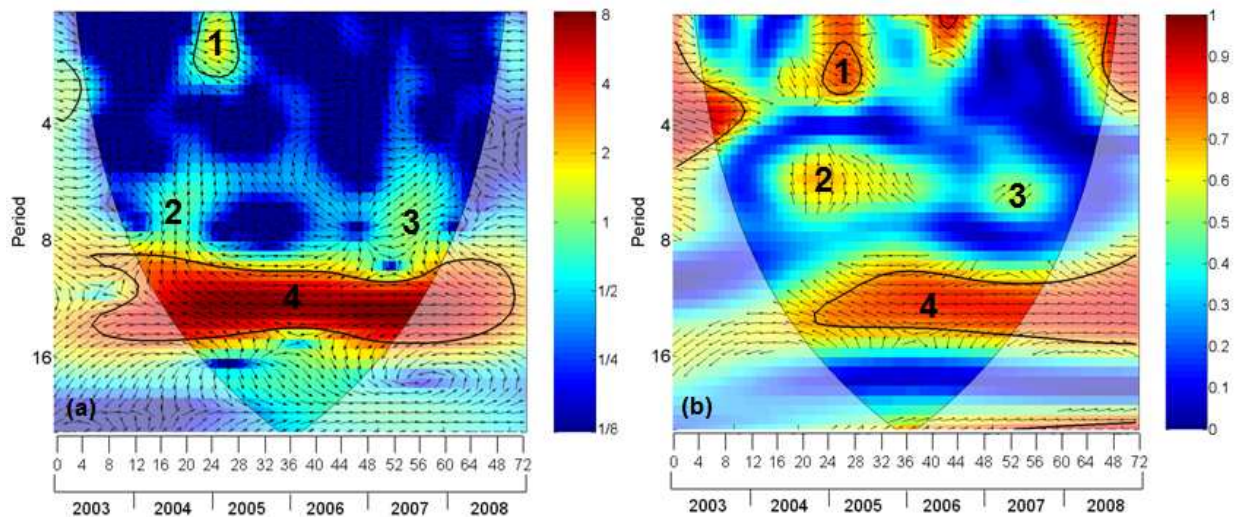

Figure 6: Cross wavelet between nighttime WST and ϕ_{lf} (a) and the coherence and phase (b).

CONCLUSIONS
The results obtained allow reaching the following conclusions:
  (1) if we assume that the water surface temperature (WST) could be explained only the heat fluxes then for daytime WST only the shortwave radiation explain 89% of the temperature variability; to nighttime WST the longwave, sensible and latent flux explain 94%;
  (2) The daytime WST and shortwave radiation presents a good agreement for periods of 6 (with shortwave retarded) and 12 months (with shortwave advanced);
  (3) For nighttime WST and longwave the good agreement is present for 1, 3, 6 and 12 months, all with longwave advanced in relation to WST;
  (4) The nighttime WST and sensible flux high common power for band periods of 2 (retarded), 6 (advanced) and 12 (advanced);
  (5) Finally, the nighttime WST and latent flux with band periods of 2 (retarded), 6 (retarded) and 12 months (WST and latent flux in anti-phase).

ACKNOWLEDGMENTS

REFERENCES
Alcântara, E., Novo, E., Stech, J., Lorenzzetti, J., Barbosa, C., Assireu, A., Souza, A. (2010). A contribution to understanding the turbidity behaviour in an Amazon floodplain, Hydrol. Earth Syst. Sci. **14**:351-364.

Bonnet MP, Poulin M, Devaux J (2000) Numerical modeling of thermal stratification in a lake reservoir: Methodology and case study. Aquatic Science **62**:105-124.

Crosman ET, Horel JD (2009) MODIS-derived surface temperature of the Great Salt Lake. Remote Sensing of Environment. **113**:73-81.

Grinsted, A., Moore, J. C., Jevrejeva, S. (2004). Application of the cross wavelet transform and wavelet coherence to geophysical time series, Nonlinaer Proc. Geoph. **11:**561–566.

Henderson-Sellers B (1986) Calculating the Surface Energy Balance for Lake and Reservoir Modeling: A Review. Reviews of Geophysics. **24**:625-649.

Jerosch, K., Schlüter, M., Pesch, R. (2006). Spatial analysis of marine categories information using indicator Kriging applied to georeferenced video mosaics of the deep-sea H˚akon Mosby Mud Volcano, Ecol. Inform. **1**:391-406.

Oesch D, Jaquet J-M, Hauser A, Wunderle S (2005) Lake surface water temperature using advanced very high resolution radiometer and moderate resolution imaging spectroradiometer data: validation and feasibility study. Journal of Geophysical Research, **10**(C12014):1-17.

Oesch D, Jaquet J-M, Klaus R, Schenker P (2008) Multi-scale thermal pattern monitoring of a large lake (Lake Geneva) using a multi-sensor approach. International Journal of Remote Sensing. **29**:5785-5808.

Reinart A, Reinhold M (2008) Mapping surface temperature in large lakes with MODIS data. Remote Sensing of Environment. **112**:603-611.

Torrence, C., Webster, P. (1999) Interdecadal changes in the ENSO-Monsoon system. Journal of Climate. 12:2679-2690.

Wan, Z. (2008). New refinements and validation of the MODIS land-surface temperature/emissivity products. Remote Sensing of Environment. **112**:59-74.